ROCK RECOGNITION USING FEATURE CLASSIFICATION

R C Crida and G de Jager
University of Cape Town, Faculty of Engineering, Digital Image Processing Laboratory,
Private Bag, Rondebosch 7700, SOUTH AFRICA
Email: rcrida@dip1.ee.uct.ac.za

Abstract —
A knowledge based approach to finding fixed size rocks within an image is described. It is intended to be a building block within a multiresolution system. Each point is hypothesised to be a rock and a region surrounding it is labelled using knowledge of rock characteristics. Twelve features are then measured and used to test the hypothesis by means of a combination of thresholding and k-nearest-neighbour classification.

I Introduction

Measurement of rock size distribution or fragmentation has application in the mining industry where sophisticated control systems are used to monitor and control autogenous mills. The use of image processing as a non-invasive measurement technique offers advantages over conventional techniques such as: undisturbed feed monitoring and repeatble results. Hunter et al [1] gives an overview of image processing techniques for measuring fragmentation. See McDermott and Miles [2], Ivanov et al [3] and Berger [4] for further examples.

This paper describes a knowledge based approach to determining the position of fixed size rocks within an image. This solution is being used as a building block within a larger multiresolution system for measuring fragmentation using image processing. To take advantage of the multiresolution approach, all processing has been matched to a particular size of object, later referred to as the optimal size. The radius of an optimally sized disc will be referred to as the optimal radius. For a similar approach using neural networks see Crida [5]. The system described here will attemp to detect rocks at each level in a multiresolution image pyramid and compile a list of detected rocks from which the size distribution can be calculated.

Although time consuming, this approach to the problem is more robust and accurate than more direct techniques which attempt to measure a size distribution directly by means of chord measurements [6]. In addition the performance is more easily verified since each rock identified by the system can be selected and highlighted on an image.

The process of detecting optimally sized rock will be referred to as the system. The system described here uses knowledge of rock images to postulate rules which are appropriate when an optimally sized rock is present in the region of interest. In the first part of the system, it is initially hypothesised that each point in the image is the centre of an optimally sized rock. The rules are then used to determine the extent of a blob in a region of interest around each point by locking onto image features which could correspond to an optimally sized rock. A blob is defined as a bright region within the grey level image, the extent of which is the segmented region. The first part of the system is broken into three stages; blob edge detection, boundary completion and blob extent calculation. These are described in Sections II and III.

The next stage involves testing the hypothesis. A feature vector is calculated for the detected blob extents and classification is performed to decide if the rules were valid for that particular region of interest. Feature calculation and the method of classification are described in Section IV.

Results and conclusion are given in Section V and VI respectively.

II Edge Detection

A region of interest R is defined as a square subimage centred on the selected point of interest. The distance to the edge of the square is 1.5 times the optimal rock radius. R is made larger than the object to be detected to provide some contextual information or 'peripheral vision' to the detection process. Detecting a rock involves determining which edges in R could belong to a rock shaped blob. An edge detected image E is used to find the edges of rocks. Figure 1 shows an ideal and a typical edge image. With ideal edge detection, each rock is disconnected from each neighbour and there are no spurious edges within the rocks. In a typical edge image gaps appear in the rock boundaries where neighbouring rocks have merged. Internal edges appear within rocks due to surface marking and close neighbouring rock edges can confuse the detection of rock boundaries.

Several rules will be postulated which which largely overcome the problems shown in figure 1 when an optimally sized rock is present. The rules used for designing the edge detection algorithm are described next:

- *A rock is basically circular in shape.* Although not applicable to all rocks, experience has shown that with sufficient tolerance, this rule is not unjustifiable for the particular rocks that are being investigated. This very important rule allows the use of a radial edge detector for finding rock edges. The central point of R is assumed to be the middle of a

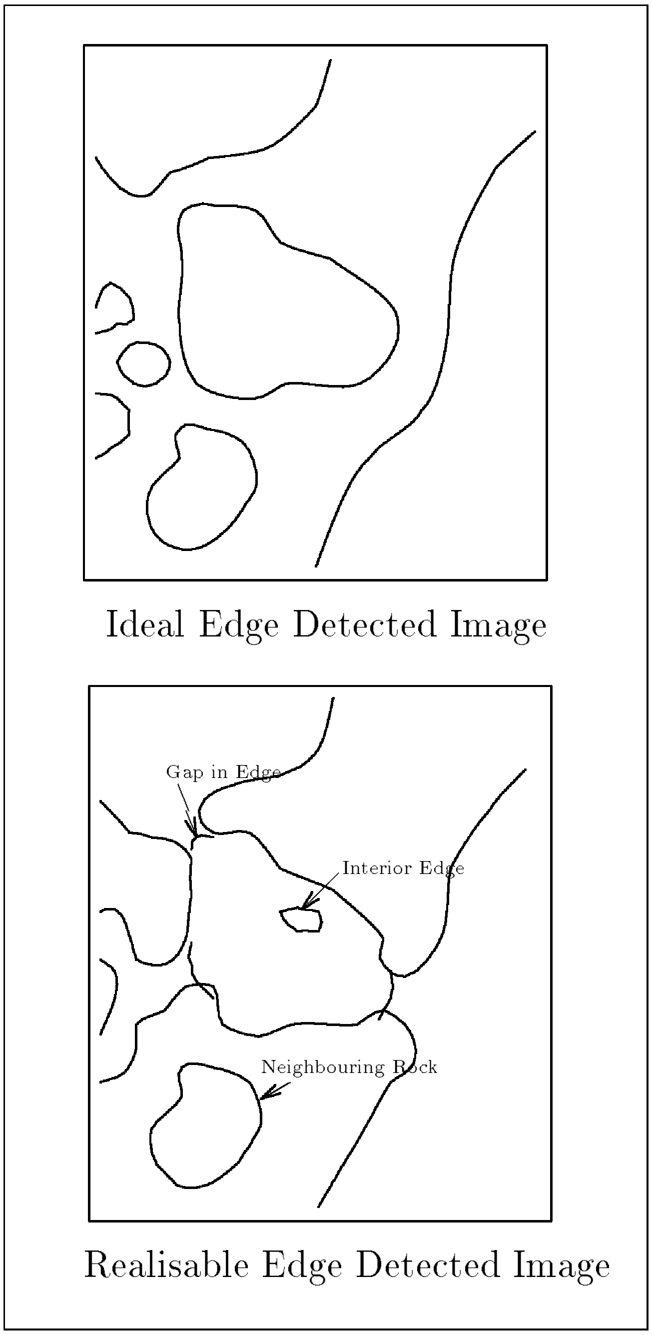

Figure 1: Ideal and typical edge images. The top diagram represents ideal edges from a rock image and the bottom image indicates the contamination that is usually present.

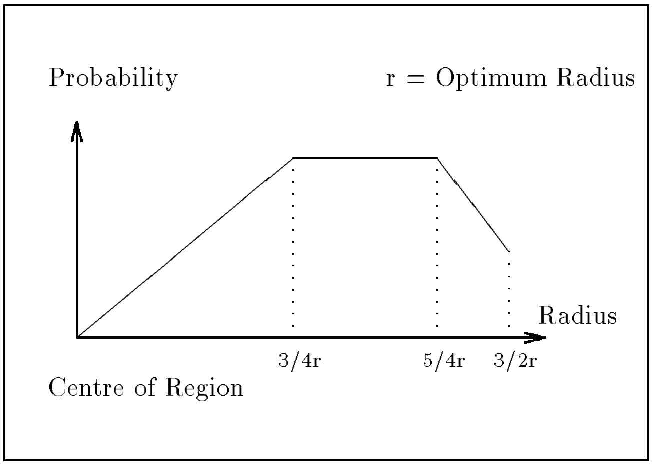

Figure 2: The rock edge probability mask is a circularly symmetric array with values which change radially as shown above.

rock and the edge strength perpendicular to radial lines is found since edge points of a circular blob could not be parallel to radial lines. Edge strength is calculated as the gradient or difference between a point and its outer neighbour on a radial line in R.

- *A rock is lighter than its background.* When rocks are illuminated with diffuse light, they cast a slight shadow which results in a dark band around each rock. Because of this, only points where the grey level is decreasing can be candidates for rock edges. This reduces the chance of confusion with neighbouring rock edges. A thresholded image T is created by determining the moment preserving threshold [7] of R. Because of the dark band, an optimally sized rock will be well preserved in the thresholded image.
- *A rock is expected to be a certain size.* Only a rock that is the optimal size need be accurately detected and so all other size objects can be ignored. Because of this and the circularity constraint, the probability P_r of finding a rock edge on a radial line will increase to the optimum radius and then decrease as shown in figure 2. A higher value of P_r indicates a greater chance of expecting a rock edge. The flat region in the middle is to allow for irregularities in the boundary shape. This rule helps to overcome the problem of holes or interior edges because if the rock is the right size, its true edge will be closer to the optimum radius and thus have a greater probability P_e of being selected.

All radial lines are now scanned for a rock edge which is defined as a positive edge strength with the greatest probability P_e where $P_e = E(x,y) * P_r(\sqrt{x^2+y^2})$. (x,y) is relative to the point of interest on the radial line therefore $\sqrt{x^2+y^2}$ is the distance from the centre of the region of interest to (x,y).

The detected radii are stored in a list. For those radial lines that have no suitable edge points, a zero is stored in the list. These gaps in the detected edge will be dealt

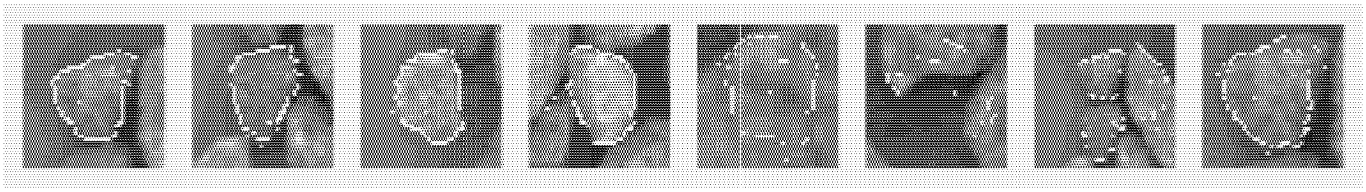

Figure 3: 8 example region of interest images with detected edge points superimposed are shown above. The four rock images have been accurately edge detected. The fifth and sixth images have meaningless edge points selected. The seventh largely indicates that the detected edges favour merging the rocks. The eighth has most of the true rock edge points except in the top right corner where the probability has decreased due to the rock's size.

with in section III.

Figure 3 shows edges that have been detected for several sample subimages. The first four images contain optimal rocks; the fifth shows a very close view of a rock; the sixth shows the edges of two rocks; the seventh shows a cluster of rocks and the eighth is an oversized rock. It can be seen from this figure that where there is an optimally sized rock, almost all edge points detected are in fact true rock edge points belonging to this rock.

III Blob Extent

The list of most probable edge points found in the previous section has two problems, missing and spurious edge points. Both of the problems are tackled using the following rule:

- *A rock has a continuous boundary.* Due to physical constraints, any step discontinuity in the edge is an error and where there are gaps, they should be filled.

To tackle the discontinuity problem, the list of radii is scanned for outliers which are defined as single points with both neighbours more than a fixed distance away. These points are removed from the list and become gaps. If a point is adjacent to a gap, the value at the other side of the gap is taken as the neighbour.

Gaps in the radii list are then filled in using linear interpolation of the radius between the edge points of each gap. This method satisfies both the continuity and circularity rules.

Figure 4 shows the resulting rock boundaries after appling the previous two methods to the radii lists. The examples show that where there is an optimal rock, a continuous and localised boundary of the rock has been detected. All outliers have been successfully removed from the rock images. The beneficial effect of gap interpolation is most evident in the fourth image where a gap has been filled at the upper left side of the rock. In the case of the images not containing rocks, the boundary detection has generally resulted in a discontinuous line which can be detected later.

The complete extent of the rock is now determined using the continuous radii list. This is achieved by drawing radial lines in a blank array to the distance specified in the radii list for each direction. Due to quantisation problems, holes can appear in the resulting array which must be passed through a hole filling filter to satisfy the following rule:

- *A rock is simply connected.* Since the rocks of interest do not have holes in them, this rule can be applied. A hole filling filter — which sets all points with more than five of its 8-connected neighbours are set — is used to fill any small holes that appear in the detected rock extent.

Figure 5 shows the result of superimposing the extent of each rock on the subimage. The blob extent algorithm has produced for each case a simply connected region. Where a rock is present, it has been accurately segmented and has a continuous boundary. Where no suitable rock is present, the boundary is more convoluted, has more discontinuities and the area is more variable. These differences can be detected using feature vector classification.

IV Feature Calculation

A statistical pattern recognition approach has been taken to perform classification. Bartlett et al [8] describe a visual inspection system which uses statistical pattern recognition. They highlight the necessity of selecting good features to ensure the success of any classification algorithm. They describe good features as having the following characteristics:

- They can be calculated reasonably quickly.
- Values for the features should cluster together for each of the different classes.
- The clusters of values for different classes should be spaced far apart.

Twelve features have been developed for use in this system. They were chosen based on intuition after inspection of the images being classified and then refined through interaction. The characteristics of good features were kept in consideration and all the features selected have been normalised to the range 0–1. The following list gives a brief description and motivation for each of the features.

1. *Proportion of good points.* This is the proportion of defined points in the radii list after outliers have been removed and before gaps are filled. Only edge points with a strength greater than one quarter the

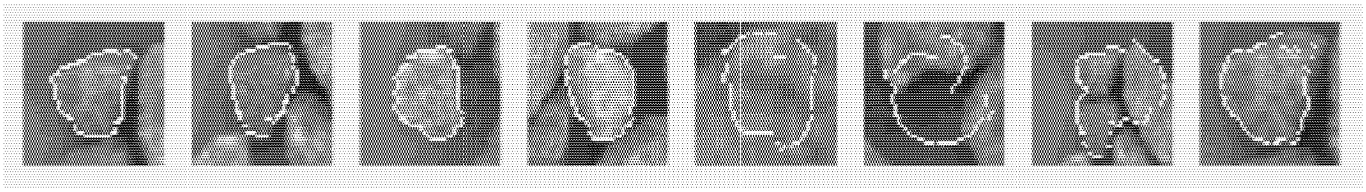

Figure 4: The 8 example images with detected boundary points superimposed are shown above. All outliers have been removed from the first four pictures. Gap interpolation has been successful in the fourth picture at the upper left. The cluster of rocks has been merged by the resulting boundary while the other boundaries are fairly discontinuous.

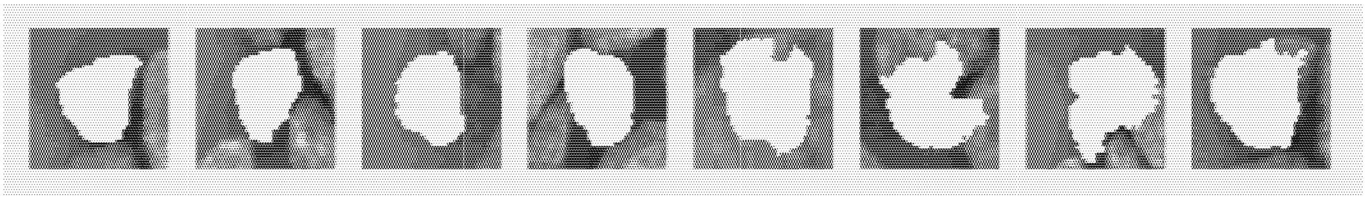

Figure 5: The 8 example images with detected extent points superimposed. In each case a simply connected region has been labelled in accordance with the rule. In the first four pictures, the rocks have been accurately segmented. Several features of the detected regions in the remaining four pictures make them stand apart from the first four. These include more discontinuous boundaries, a lower circularity and more variable area. These features can be used to classify the detected blob as representing an optimal rock or not.

maximum value are kept. A high proportion is desirable since it indicates the presence of a complete edge in the image.

2. *Surface area of blob* is the number of pixels enclosed by the detected blob boundary as a proportion of the optimal area minus 0.5. The optimal area is that of an optimally sized disc. A value near 0.5 is desirable as it indicates a blob with a near optimal area.
3. *Boundary strength over interior strength* is the average boundary edge strength, divided by the average internal edge strength. A high value is desirable as one would expect the gradient to be stronger at the edge of a rock than in its interior.
4. *Circularity.* The circularity is defined as $Circularity = \frac{4\pi Area}{Perimeter^2}$. This value is unity for a circle and decreases as the boundary increases in complexity. A high value is desired because rocks are expected to be roughly circular.
5. *Centre of mass offset.* The offset is defined as $Offset = \sqrt{\overline{x}^2 + \overline{y}^2}$ where $\overline{x}$ and $\overline{y}$ are the zero order moments of the detected blob extent. This feature measures the distance from the centre of R to the centre of mass of the blob.
6. *Largest boundary gap size* is measured as the length of the longest gap in the radii list after outlier removal and before interpolation as a proportion of the blob perimeter. A low value is desirable because a rock should not have large gaps in it boundary. This feature can prevent the corners of large rocks being mistaken for small rocks, ie rock splitting.
7. *Proportion of background.* This is calculated as the proportion of pixels in T that are above the threshold within the extent of the blob to the measured area. A high value is desirable because rocks should be preserved in T.
8. *Edge position probability.* This is the average value from the probability mask of the boundary points of the blob. It gives a measure of how close the boundary is to the optimal radius.
9. *Edge strength.* This is the average value of E for each boundary point of the blob plus 0.5 since gradient can be negative.
10. *Edge discontinuities* is the number of boundary discontinuities as a proportion of the boundary length. A discontinuity is defined as a step change of greater than 1 pixel.
11. *Maximum gap strength.* A gap detected image G is calculated by applying the morphological tophat function to a photometrically inverted R. The filter highlights narrow dark gaps between close rocks and is used to reduce the chance of merging rocks. This feature is calculated as the maximum value of the highlighted gap subimage within the interior of the blob, not including the edge points. A high value for this feature indicates a gap within the blob which gives a strong evidence for rock merging.
12. *Minimum edge strength.* The edge strengths from each point on the boundary are compiled into a list which is a circular signal representing the boundary edge. This signal is eroded with a narrow structuring element to remove narrow high spikes. It is then dilated using a wider structuring element to fill in the low regions. If there is a wide low region it will survive this process. Narrow low regions will be filled in by the dilation. The minimum value of the signal is taken as the feature value. A low value indicates the presence of wide low regions in the boundary edge strength. This is used to help prevent rock splitting.

Feature	*Allowed range for rock*
1	> 0.6
2	0.25–0.5
3	0.58–0.66
4	> 0.7
5	< 0.2
6	< 0.2
7	0.45–0.8
8	> 0.8
9	0.55–0.65
10	0.15–0.5
11	< 0.15
12	> 0.1

Table 1: Threshold limits for features representing rocks.

Table 1 gives list of threshold limits for each of the features. A training set and test set have been constructed by providing the correct classification for feature vectors through manual inspection of their corresponding regions of interest. The thresholds have been determined from a training set to ensure that no rocks are misclassified.

The measurement of these features results in a 12 dimensional feature vector in multidimensional space. The problem of classifying the feature vector involves partitioning the 12D space into two regions, in this case; a region for features representing rocks and the remainder for features which don't represent rocks. Many possible classification techniques could be used to perform the partitioning, but a combination of approaches has been developed for speed of execution.

Initially, the feature vector is classified using the thresholds in table 1. All feature vectors representing a rock should pass this test along with some representing non-rocks. Feature vectors with extreme values will be rejected and classified as non-rocks at this stage. The remaining vectors are checked again using a k-Nearest-Neighbour classifier which requires a design set of sample feature vectors with their true classification.

V Results

The measured feature values for the 8 example region of interest images are presented in table 2. In the final column, an R indicates classification as a rock picture and N indicates that it is not a rock picture. For the non-rock pictures, the number following the N is the first feature number that exceeded the threshold limits in the first stage of classification. In other words, the first and fourth non-rock pictures failed because their area was too high, the second failed because too few edge points were found and the third failed because there was too much edge information within the interior of the detected blob.

In each case, more than one feature would have failed the non-rock feature vectors. This redundancy should make the system more capable of classifying correctly under marginal conditions.

Figure 6 gives an impression of the overall performance of the combinational classification approach. The graph shows traces from two methods of classification. The first trace is the result of k-Nearest-Neighbour classification only. The remaining five traces were generated using the combination of thresholding and k-Nearest-Neighbour classification. The figures quoted in the legend of the graph indicate how the thresholds have been calculated. The thresholds have been determined in such a way that the given proportion of the rock feature vectors will pass the test. This has been done to reject some of the extreme rock feature vectors which could be erroneous.

It can be observed from this graph that for the case where the proportion of rocks accepted by the threshold is 1.00, there is no compromise to the classification performance while there is an appreciable increase in average speed of classification. In addition, classification accuracy increases with an increase in k.

VI Conclusions

The good results achieved depend on three basic factors in classification, all of which appear to perform accurately. They are:

- The knowledge based region of interest analysis rules gives an accurate segmentation when a rock is present.
- The 12 features appear to be reasonably robust basis for classification as at least one feature will have an extreme value for any non-rock region of interest.
- The combination of two classification techniques produces no drop in performance and a large improvement in average speed.

As a result of the good performance, this method for detecting rocks should perform well in a multiresolution fragmentation analysis system.

References

[1] G. Hunter, C. McDermott, N. Miles, A. Singh, and M. Scoble, "A review of image analysis techniques for measuring blast fragmentation," *Mining Science and Technology*, vol. 11, pp. 19–36, July 1990.

[2] C. McDermott and N. Miles, "The measurement of rock fragmentation using image analysis," *Departmental Magazine, Department of Mining Engineering*, pp. 49–61, 1988.

[3] E. Ivanov, W. Osten, and W. Juptner, "An image processing system for monitoring of conveyor belt systems," in *Machine Vision Applications in Industrial Inspection II*, IS&T/SPIE Symposiom on Electronic Imaging Science and Technology, SPIE, 1994.

[4] G. F.-M. Berger, "Software for a particle-size analyser based on image analysis techniques," Master's thesis, University of the Witwatersrand, 1985.

Feature	1	2	3	4	5	6	7	8	9	10	11	12	Class
Rock	1.000	0.376	0.661	0.810	0.073	0.000	0.762	0.974	0.576	0.023	0.125	0.500	R
	0.940	0.343	0.673	0.818	0.200	0.034	0.607	0.914	0.570	0.011	0.195	0.333	R
	0.950	0.364	0.702	0.834	0.045	0.034	0.846	0.972	0.608	0.000	0.184	0.333	R
	0.900	0.383	0.676	0.826	0.107	0.057	0.807	0.956	0.651	0.000	0.199	0.360	R
Non	0.740	0.572	0.722	0.636	0.158	0.069	0.743	0.988	0.522	0.034	0.070	0.000	N2
Rock	0.380	0.497	0.698	0.572	0.026	0.368	0.381	0.969	0.518	0.034	0.105	0.000	N1
	0.650	0.487	0.674	0.608	0.259	0.149	0.663	0.891	0.546	0.057	0.324	0.267	N3
	0.980	0.541	0.676	0.667	0.130	0.011	0.857	0.994	0.563	0.046	0.145	0.500	N2

Table 2: Table of feature values

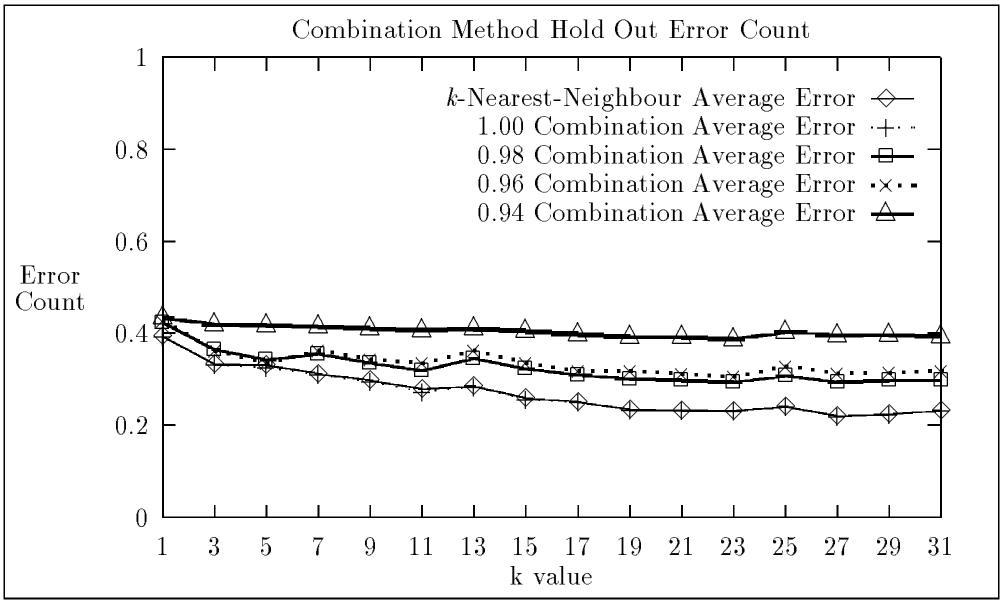

Figure 6: Graph of Error Count vs k value for the combination classification rule using Hold Out method. The average Error Count is shown for each threshold level.

[5] R. Crida, "Rock recognition using neural networks," *Third South African Workshop on Pattern Recognition*, November 1992.

[6] T. Lange, *Measurement of the size distribution of rocks on a conveyor belt using machine vision*. PhD thesis, University of the Witwatersrand, 1990.

[7] W.-H. Tsai, "Moment-preserving threshold: A new approach," *Computer Vision, Graphics, and Image Processing*, no. 29, pp. 377–393, 1985.

[8] S. L. Bartlett, P. J. Besl, C. L. Cole, R. Jain, D. Mukherjee, and K. D. Skifstad, "Automatic solder joint inspection," *IEEE Transactions on Pattern Analysis and Machine Intelligence*, vol. 10, pp. 31–43, January 1988.